RSC Advances

PAPER

View Article Online
View Journal | View Issue

Cite this: *RSC Adv.*, 2025, **15**, 40279

Influence of polyethylene glycol on the mucus penetration and stability of lipid nanoparticles in cryopreservation and lyophilization

Xueyan Wang,[a] Yayi Zhao,[a] Xingtao Huang,[b] Yu Huang,[b] Ye Zhang [c] and Chenjie Xu *[a]

Received 24th July 2025
Accepted 15th October 2025

DOI: 10.1039/d5ra05353f

rsc.li/rsc-advances

Lipid nanoparticles (LNPs) have emerged as clinically validated drug delivery vehicles, as demonstrated by the successful deployment of COVID-19 mRNA vaccines (Comirnaty and Spikevax) and siRNA therpy (Patisiran). Building on these achievements, we investigated the functional roles of free polyethylene glycol (PEG) molecules in optimizing LNP performance. This study focused on enhancing mucus penetration capability and maintaining storage stability under various storage conditions. We found PEG molecules (MW 400–6000 Da) significantly improved LNP penetrate through mucosal barriers, with PEG 2000 demonstrating optimal penetration efficiency. Stability assessments showed that LNPs remained stable in PEG media at −20 °C for 4 weeks. However, none of the tested PEG formulations prevented LNPs aggregation during lyophilization.

Introduction

Lipid nanoparticles (LNPs) have emerged as ideal carriers for nucleic acid therapeutics,[3] offering enhanced drug stability, prolonged half-life, and improved transmembrane transport.[4] These properties have been critical to the success of COVID-19 mRNA vaccines (Comirnaty and Spikevax)[1] and siRNA medicine (Parisian).[2]

A key component in optimizing LNP performance is polyethylene glycol (PEG), a hydrophilic non-ionic polymer widely used as a stealth polymer by covalently modifying the surface of nanoparticles including LNPs. PEG confers several advantages, including prolonged circulation time, reduced immunogenicity, and altered pharmacokinetic profiles.[5] Furthermore, PEG enhances LNP solubility and minimizes protein adsorption by forming a hydrated polymer layer around the nanoparticles.[6] This protein-repellent property also facilitates mucus penetration,[7] with performance dictated by PEG molecular weight,[8] chain length,[9] and coating density.[10] Beyond its role in drug delivery, PEG serve as an effective cryoprotectant for various biological entities, including bacteriophages,[11] microorganisms,[12] and single cells[13] and cell spheroids.[14] While the underlying mechanisms remain incompletely understood, PEG's cryoprotective efficacy is strongly molecular-weight-dependent.[13] Studies suggested that PEGs with molecular weight of 400 and 600 enter cells through diffusion and inhibit intracellular ice formation, whereas PEGs with molecular weight of 10 000 and 20 000 promote cellular dehydration *via* osmotic pressure, thereby reducing ice crystal formation.[13,15,16]

Given these benefits, significant efforts have focused on developing novel PEG derivatives and conjugation strategies to optimize LNP formulations. However, one overlooked area is the potential influence of free PEG in LNP dispersion media on mucus penetration and storage stability. While LNPs modified with a high density of low-molecular-weight PEG can be efficiently transported across mucus, can LNPs surrounded by the large amount of free PEG do the same? Additionally, current LNP-based vaccines (*e.g.*, Comirnaty and Spikevax) rely on sucrose as a cryoprotectant for frozen storage.[1] Given PEG's known cryoprotective properties, can it help maintain the stability of LNP formulations in both dry and wet conditions?

To answer these questions, we prepared a series of cryogenic media containing PEGs of varying molecular weights. LNPs, synthesized *via* microfluidic, were dispersed in these formulations, and their mucus-penetrating capacity were evaluated. Subsequently, we assessed the stability of LNPs after long-term storage at 4 °C, −20 °C, and −80 °C by monitoring particle size changes. Finally, we investigated the impact of PEG-containing media on LNP stability during freeze-drying (lyophilization).

Material and methods

(2,3-Dioleoyloxy-propyl)-trimethylammonium-chloride (DOTAP) (Pharmaceutical Grade), DSPE-PEG2000

[a]*Department of Biomedical Engineering, College of Biomedicine, City University of Hong Kong, Tat Chee Avenue, Kowloon Tong, Hong Kong SAR, P. R. China. E-mail: chenjie.xu@cityu.edu.hk*

[b]*Department of Biomedical Science, College of Biomedicine, City University of Hong Kong, Tat Chee Avenue, Kowloon Tong, Hong Kong SAR, P. R. China*

[c]*Active Soft Matter Group, Songshan Lake Materials Laboratory, Dongguan, Guangdong Province, 523808, China*

(Pharmaceutical Grade), and 1,2-Dipalmitoyl-*sn*-glycero-3-phosphorylcholine (DPPC) (Pharmaceutical Grade) were purchased from AVT (Shanghai) Pharmaceutical Tech Co. Ltd. Cholesterol (Pharmaceutical Grade), PEG 400 (Reagent grade), PEG 800 (Reagent grade), PEG 1000 (Reagent grade), PEG 2000 (Reagent grade), PEG 4000 (Reagent grade), PEG 6000 (Reagent grade), PEG 10 000 (Reagent grade). FITC-Dextran (average molecular weight 250 000) and mucin (type III) were purchased from Sigma. Hoechst (33 342), Dulbecco's Modified Eagle Medium (DMEM, Gibco), fetal bovine serum (FBS) and penicillin-streptomycin were purchased from Thermo Fisher Scientific. 12-well Transwell Plates were acquired from NEST. Human Embryonic Kidney 293 cells (HEK293 cells) were generously provided by Prof. HUANG Jiandong's Lab at The University of Hong Kong, Hong Kong.

Synthesis and characterization of LNPs

LNPs were synthesized using a microfluidic device (Suzhou Zhongxin Qiheng Scientific Instrument Co., Ltd). The lipid phase consisted of DOTAP, DSPE-PEG 2000, DPPC, and cholesterol dissolved in ethanol at a molar ratio of 30 : 2 : 18 : 50. The aqueous phase comprised either 3 mg/mL FITC-dextran (as a model drug) in pure citrate buffer (pH 6.0) or pure citrate buffer (pH 6.0) for blank LNPs. The lipid and aqueous phases were mixed at a flow rate ratio of 1 : 3 (lipid : aqueous) to form LNPs, which were subsequently purified by dialysis against PBS (pH 7.4) at 4 °C. The morphological characteristics was examined using a transmission electron microscope (TEM, Hatichi HT7700, Japan) with a negative staining method involving 2% (w/v) phosphotungstic acid. Particle size and zeta potential were measured using Nanoparticle Tracking Analyzer (NTA; Zeta-View®, Particle Metrix, Germany). All experiments were performed in triplicate ($n = 3$).

LNP penetration through mucus layers

Simulated mucus was prepared by dissolving mucin (5% w/v) in PBS. Then, 50 μL of the simulated mucus onto the membrane of the insert well of a Transwell plate, while 500 μL PBS was added to the receiving well. To evaluate mucus penetration, LNPs (5×10^{10} particles/mL) were suspended in PBS containing 2.5% w/v PEG of varying molecular weights (MW: 400, 800, 1000, 2000, 4000, 6000, 10 000 Da). Next, 100 μL of each LNP suspension was added to the insert well. After incubation in a shaking incubator for 2 hours at 37 °C, the solution from the receiving well was collected and quantified using a Microplate Reader (Synergy™ H1, Agilent BioTek, USA). Mucus thickness was adjusted by changing the volume of amount of simulated mucus.

Cellular uptake of LNPs

HEK293 cells were cultured in DMEM supplemented with 10% FBS and 1% penicillin-streptomycin at 37 °C with 5% CO_2. LNPs suspended in the PEG media were then added to the cell culture media for 2 hours. After incubation, cellular uptake was observed using a confocal laser scanning microscope (Leica TCS SP8 Confocal Microscope System) and were harvested and analyzed *via* flow cytometry (BD FACSVerse™).

Stability study of LNPs stored in PEG media

LNPs (5×10^{10} particles/mL) were dispersed in 2.5% w/v PEG media of varying molecular weights and stored under different conditions. Later, the LNP solutions thaw in a 37 °C water bath before the particle size was measured by ZetaView®. The storage conditions included 4 °C, −20 °C, and −80 °C for 1 day, 1 week, 2 weeks, and 4 weeks. Samples stored at −20 °C and −80 °C were thawed in a 37 °C water bath before analysis. Particle size was measured post-thawing using ZetaView®.

Stability study of LNPs during freeze-drying

LNPs (5×10^{10} particles/mL) in 2.5% w/v PEG media were frozen in −20 °C overnight following by lyophilization. The lyophilized samples were stored at 4 °C for different times (1 day, 1 week, 2 weeks, and 4 weeks). After storage, LNPs were reconstituted in deionized water and particle size was assessed using ZetaView®.

Results

LNP penetration through mucus in PEG media

The synthesized LNPs, prepared *via* microfluidic assembly, exhibited an average hydrodynamic diameter of 110 nm and a zeta potential of +19.04 mV (Fig. 1B). To evaluate mucus penetration capability, we established an invitro mucus model by depositing 50 μL of simulated mucus (5% w/v) on Transwell insert well, forming a uniform mucus layer approximately 446 μm thick (Fig. 1A). We assessed the effect of PEG molecular weight on LNP penetration by dispersing LNPs in PBS containing different PEGs (MW = 400, 800, 1000, 2000, 4000, 6000, 10 000 Da). LNPs in PBS solution acted as the control group. After 2 hours incubation, fluorescence quantification of the receiving well revealed that all PEG except PEG 10,000 enhanced LNP transport through the mucus barrier compared to PBS controls (Fig. 1C). We hypothesize that the long chain of PEG 10,000 may cause its entanglement with mucin fibres, thereby hindering the LNP penetration.

PEG 2000 demonstrated optimal penetration enhancement (Fig. 1C) and was selected for further characterization. When testing mucus layers of varying thickness (2000–8000 μm), we observed an inverse relationship between mucus thickness and LNP penetration efficiency at fixed incubation time (2 hours) (Fig. 1D). Conversely, with constant mucus thickness (446 μm), penetration efficiency increased with incubation time until reaching equilibrium at 3.5 h (Fig. 1E).

The functional delivery capability of mucus penetrating LNPs was confirmed through cellular uptake studies in HEK293 cells. After incubation with FITC Dextran-LNPs, confocal microscopy imaging revealed effective internalization of PEG 2000-mediated LNPs, as evidenced by green fluorescence, while no signal was detected in the PBS control group (Fig. 2A). Flow cytometry analysis revealed that PEG 2000-mediated penetration resulted in 5.74% FITC-positive cells, representing

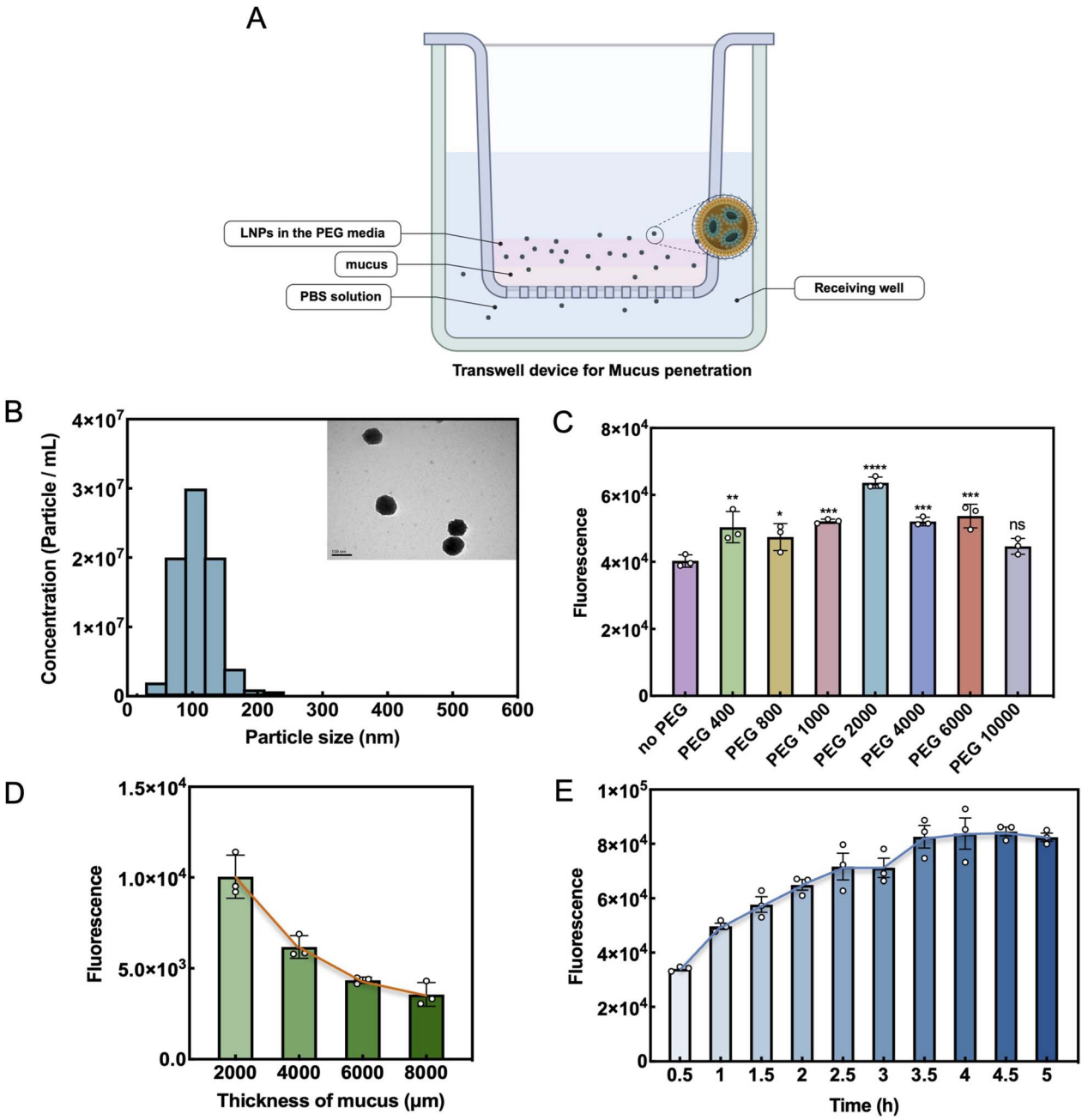

Fig. 1 Mucus penetration of LNPs in the PEG media: (A) illustration of mucus penetration model in the Transwell device. (B) Representative TEM image and size histogram from NTA measurement of LNPs. (C) LNP penetration through the mucus layer in PBS and PEG media (MW = 400, 800, 1000, 2000, 4000, 6000, 10 000 Da). Statistical differences in C were determined with a one-way ANOVA, $P < 0.0001$. (D) LNP penetration through the mucus layer with different thickness in PEG 2000 medium. Statistical differences in D were determined with a one-way ANOVA, $P < 0.0001$. (E) LNP penetration through mucus layer in PEG 2000 medium in the period of 5 hours. Statistical differences in E were determined with a one-way ANOVA, $P < 0.0001$. Data in (B)–(D) was presented as mean ± s.d, $n = 3$.

a significant improvement over PBS controls (Fig. 2B and C). Cells exposed to PEG 2000-mediated LNPs exhibited 2.67-fold greater mean fluorescence intensity than PBS controls (Fig. 2D). As expected, direct application of LNPs (positive control) yielded higher fluorescence signals than mucus-penetrated samples, suggesting partial LNPs retention in the mucus layer.

Stability of LNPs in PEG media

We evaluated the stability of LNPs in various PEG media (MW = 400, 800, 1000, 2000, 4000, 6000, 10 000 Da) under different temperatures (4 °C, −20 °C and −80 °C) for 1 day, 1 week, 2 weeks and 4 weeks. Particle size changes were monitored as the primary stability indicator (Fig. 3). At 4 °C, all LNP formulations (including PBS controls) demonstrated gradual particle size

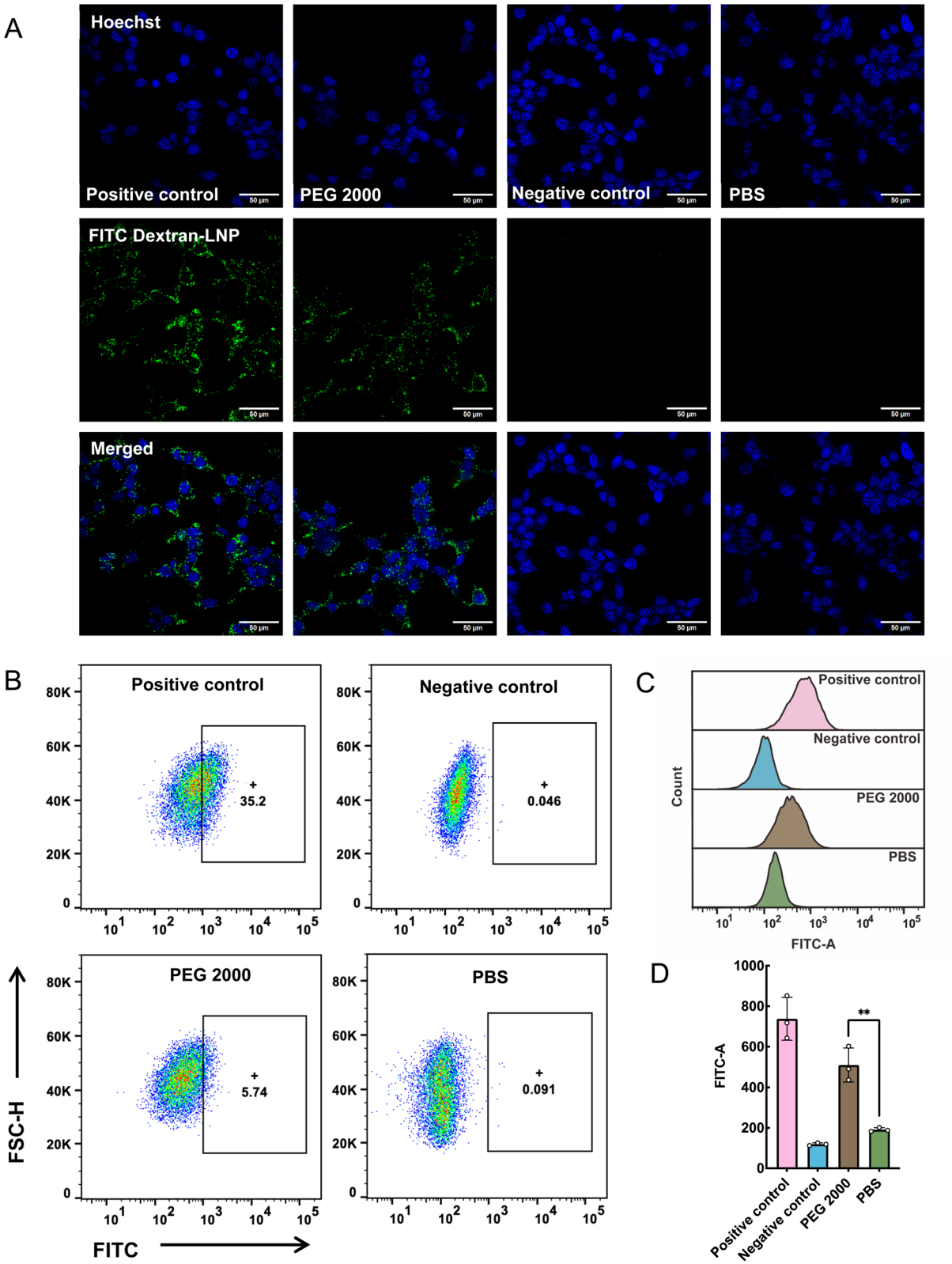

Fig. 2 Cellular uptake of FITC Dextran-LNPs in HEK293 cells. HEK293 cells treated with LNPs before penetrating through mucus (positive control), without treated with LNPs (negative control), treated with LNPs in PEG 2000 after penetrating through mucus (PEG 2000) and treated with LNPs in PBS solution after penetrating through mucus (PBS). (A) Representative confocal images of intracellular uptake of FITC Dextran-LNPs. Cell nucleus was stained with Hoechst (blue). (B) The percentage of FITC+ HEK293 cells treated with FITC Dextran-LNPs. (C) Flow cytometry histogram of cellular uptake of FITC Dextran-LNP in HEK293 cells. (D) Quantitative analysis of fluorescence intensity of FITC in HEK293 cells. Data in C was presented as mean ± s.d, $n = 3$. Statistical differences in D were determined with a two-way ANOVA, $^{**}P < 0.01$.

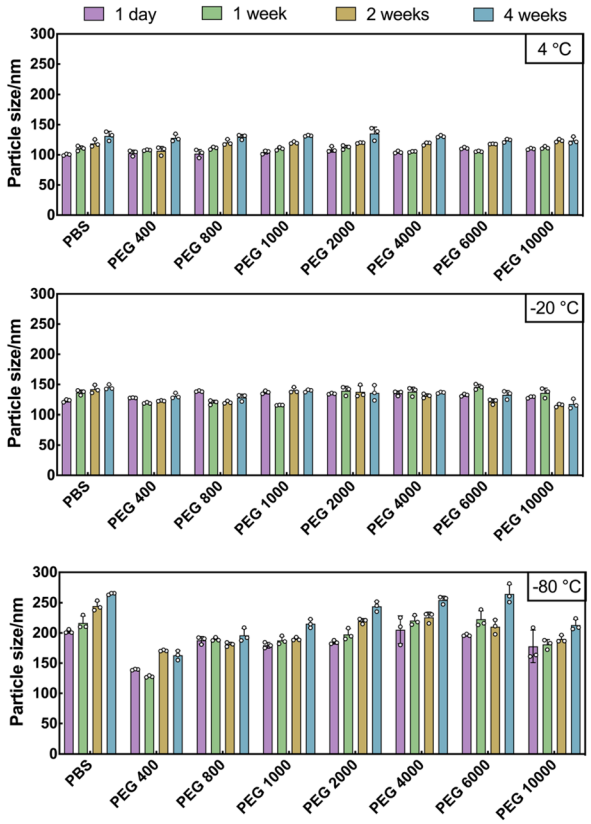

Fig. 3 Particle size of LNPs after storage at different temperature (4 °C, −20 °C, −80 °C) and different times (1 day, 1 week, 2 weeks, 4 weeks). (B–D) Particle sizes of LNPs in PEG media with different molecular weight (MW = 400, 800, 1000, 2000, 4000, 6000, 10 000 Da) in 1 day, 1 week, 2 weeks, 4 weeks with the storage temperature (B) 4 °C; (C) −20 °C; (D) −80 °C. Data in B–D was presented as mean ± s.d. $n = 3$. Statistical differences in B–D were determined with a two-way ANOVA.

increases throughout the storage period, consistent with established LNP storage limitations. In contrast, −20 °C storage maintained excellent stability, with PEG-formulated LNPs showing minimal size variations during the 4-week observation period. Notably, −80 °C storage induced substantial particle aggregation across all PEG formulations, although PEG 400 exhibited relative protective effects.

During the freezing process, the formation of ice crystals inside and outside the LNPs damages the membranes. The concentration of the components increases, which reduces the distance between the particles and causes aggregation. The change in osmotic pressure also causes membrane damage. The enhanced damage at −80 °C *versus* −20 °C likely results from increased interfacial area and smaller ice crystal formation characteristic of rapid freezing. Importantly, while all PEG formulations aggregated at −80 °C, their performance still surpassed PBS controls, confirming PEG's partial cryoprotective capacity.

Stability of LNPs in PEG media during the lyophilization

Building on these findings, we investigated lyophilization stability using −20 °C as the optimal pre-freezing condition.

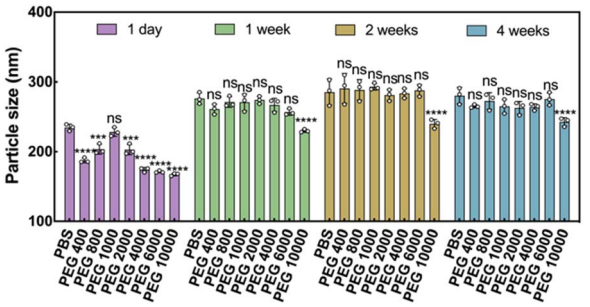

Fig. 4 Changes in particle size of LNPs after freeze-drying and storage at 4 °C for 1 day, 1 week, 2 weeks, and 4 weeks. Significant differences in the graphs were obtained in comparison with the group without the addition of PEG. Data was presented as mean ± s.d, $n = 3$. Statistical differences were determined with a two-way ANOVA, ns = non-significant, *$P < 0.05$, **$P < 0.01$, ***$P < 0.001$, ****$P < 0.0001$.

Later, the LNP power was storage under 4 °C for 1 day, 1 week, 2 weeks, 4 weeks (Fig. 4). Post-lyophilization analysis revealed that while most formulations maintained sub-200 nm particle sizes initially (day 1) significant aggregation occurred by week 1 of storage at 4 °C. No significant difference was observed between LNPs in different PEG media except for PEG 10 000. This rapid destabilization suggests that lyophilization-induced dehydration critically disrupts the electrical double layer stabilization mechanism of LNPs. The comparable aggregation profiles across most PEG molecular weights indicate that the freeze-drying process overrides the stabilizing effects observed in liquid-phase storage conditions.

Discussion

Mucus serves as a critical biological barrier, forming a viscoelastic adhesive gel that protects exposed epithelial surfaces in multiple organ systems including the respiratory, gastrointestinal, female reproductive tracts, and the surface of the eyes, by lubricating surfaces and capturing and removing foreign particles.[17] Mucus adheres and blocks foreign matter through hydrophobic, electrostatic, and hydrogen bonding interactions, presents a significant challenge for drug and gene delivery to mucosal surfaces. Our findings demonstrate that free PEG molecules in LNP formulations can effectively enhance mucus penetration, with PEG 2000 showing optimal performance.

The observed molecular weight dependence of PEG's penetration-enhancing effects likely relates to chain length interactions with mucin fibers. While molecular weight PEGs (400–6000 Da) facilitated LNP transport, PEG 10 000 showed minimal effect. The interpenetrating polymer network (IPN) effect between PEG chains and the mucus network also contributes to PEG's mucus adhesion. Coating particles with a dense layer of low-MW PEG effectively reduces hydrophobic interactions, hydrogen bonding, and IPN effects to below the threshold level required for particle slowing and immobilization. The IPN effect is stronger with higher-MW PEG (>10 000 Da). PEG chains are long enough to become significantly entangled with mucus, especially in areas with high mucus fiber density.[18] In addition, higher-MW PEG exhibits more hydrogen bonding with

mucin.[19] Furthermore, we identified two critical parameters affecting LNP penetration: (1) mucus thickness showed an inverse relationship with transport efficiency, and (2) penetration followed time-dependent kinetics, reaching maximum transport at approximately 3.5 hours. As shown in Fig. 1E, the amount of LNPs gradually increased over time and reached a plateau at approximately 3.5 hours. This indicates that the penetration of LNPs through the mucus layer is a time-dependent process. On one hand, LNPs do not rapidly traverse the mucus all at once, but rather undergo gradual penetration. This behaviour supports sustained drug release and helps avoid potential toxicity caused by a sudden, massive arrival of the drug at the target site. On the other hand, the 3.5-hour timeframe is shorter than the turnover period of many mucosal surfaces in the body (*e.g.*, 5–6 hours in the stomach and about 6–7 hours in the small intestine).[20] Therefore, within one turnover cycle, the LNPs are unlikely to be cleared and have sufficient time to penetrate the mucus and reach the target tissue.

As a colloidal system, LNPs are thermodynamically unstable and tend to aggregate.[21] Our temperature stability studies revealed that −20 °C storage provided optimal conditions, maintaining LNP stability over 4 weeks. In contrast, −80 °C storage led to significant aggregation. This temperature dependence can be explained by ice crystal formation dynamics – the smaller crystals[22,23] and larger interfacial area[24] generated at −80 °C create greater mechanical stress on the LNP structure.

Lyophilization represents a promising approach for LNP stabilization during transport and storage.[25] However, our results indicate that free PEG molecules in solution cannot prevent particle aggregation during freeze-drying. This limitation suggests that while PEG enhances colloidal stability in liquid formulations, it cannot maintain particle integrity through the dehydration-rehydration process.[26] Future studies should explore alternative cryoprotectants or formulation strategies to address this challenge.

Conclusions

Our study demonstrates that free PEG molecules serve dual functions in LNP formulations: enhancing mucus penetration and maintaining colloidal stability. The study revealed significant molecular-weight-dependent effects, with PEG 2000 emerging as the most effective formulation for enhancing LNP transport across mucosal barriers. This optimal performance likely stems from an appropriate balance between chain length and mucin interaction properties. Regarding stability profiles, all PEG-formulated LNPs demonstrated excellent preservation of particle characteristics when stored at −20 °C, suggesting this temperature represents an optimal condition for maintaining LNP integrity. However, none of the tested PEG media provided sufficient protection against particle aggregation during lyophilization processes.

Author contributions

X. W., C. X., and Y. Z. conceived the idea. X. W. performed experiments and analysed the data. Y. Z. contributed to the fabrication of LNPs. X. H. and Y. H. contributed to the device use. X. W., C. X. wrote and revised the manuscript. All authors participated in the manuscript preparation.

Conflicts of interest

There are no conflicts to declare.

Data availability

The datasets generated during and/or analysed during the current study are available from the corresponding author on reasonable request.

Supplementary information is available. See DOI: **https://doi.org/10.1039/d5ra05353f**.

Acknowledgements

C. X. appreciates the supports from the General Research Fund from the Research Grants Council of the Hong Kong Special Administrative Region, China (CityU11202222, CityU11100323, CityU11101324), and the Guangdong-Hong Kong Technology Cooperation Funding Scheme fraelom Innovation and Technology Commission (GHP/066/22GD). Any opinions, findings, conclusions or recommendations expressed in this material/event (or by members of the project team) do not reflect the views of the Government of the Hong Kong Special Administrative Region, the Innovation and Technology Commission or the Innovation and Technology Fund Research Projects Assessment Panel.

Notes and references

1 J. Kim, Y. Eygeris, M. Gupta and G. Sahay, *Adv. Drug Delivery Rev.*, 2021, **170**, 83–112.
2 Y. Y. C. Tam, S. Chen and P. R. Cullis, *Pharmaceutics*, 2013, **5**, 498–507.
3 E. Blanco, H. Shen and M. Ferrari, *Nat. Biotechnol.*, 2015, **33**, 941–951.
4 L. Kou, Y. D. Bhutia, Q. Yao, Z. He, J. Sun and V. Ganapathy, *Front. Pharmacol.*, 2018, **9**, 27.
5 M. M. Wang, C. N. Wappelhorst, E. L. Jensen, Y.-C. T. Chi, J. C. Rouse and Q. Zou, *Sci. Rep.*, 2023, **13**, 16744.
6 E. Padín-González, P. Lancaster, M. Bottini, P. Gasco, L. Tran, B. Fadeel, T. Wilkins and M. P. Monopoli, *Front. Bioeng. Biotechnol.*, 2022, **10**, 882363.
7 J. T. Huckaby and S. K. Lai, *Adv. Drug Delivery Rev.*, 2018, **124**, 125–139.
8 K. Maisel, M. Reddy, Q. Xu, S. Chattopadhyay, R. Cone, L. M. Ensign and J. Hanes, *Nanomedicine*, 2016, **11**, 1337–1343.
9 E. Samaridou, N. Kalamidas, I. Santalices, J. Crecente-Campo and M. J. Alonso, *Drug Delivery Transl. Res.*, 2020, **10**, 241–258.
10 Q. Xu, L. M. Ensign, N. J. Boylan, A. Schon, X. Gong, J.-C. Yang, N. W. Lamb, S. Cai, T. Yu and E. Freire, *ACS Nano*, 2015, **9**, 9217–9227.

11 H. L. Marton, K. M. Styles, P. Kilbride, A. P. Sagona and M. I. Gibson, *Biomacromolecules*, 2021, **22**, 5281–5289.
12 M. Hasan, A. E. Fayter and M. I. Gibson, *Biomacromolecules*, 2018, **19**, 3371–3376.
13 M. Patel, J. K. Park and B. Jeong, *Biomater. Res.*, 2023, **27**, 17.
14 S. Serrati, C. Martinelli, A. Palazzo, R. M. Iacobazzi, M. Perrone, Q. K. Ong, Z. Luo, A. Bekdemir, G. Pinto and O. Cavalleri, *PLoS One*, 2020, **15**, e0224002.
15 M. C. Banker, J. R. Layne Jr, G. L. Hicks Jr and T. Wang, *Cryobiology*, 1992, **29**, 87–94.
16 L. O'Neil, S. Paynter, B. Fuller and R. Shaw, *Cryobiology*, 1997, **34**, 295–301.
17 L. M. Ensign, C. Schneider, J. S. Suk, R. Cone and J. Hanes, *Adv. Mater.*, 2012, **24**, 3887–3894.
18 Y.-Y. Wang, S. K. Lai, J. S. Suk, A. Pace, R. Cone and J. Hanes, *Angew. Chem.*, 2008, **47**, 9726.
19 K. Nakamura, Y. Maitani, A. M. Lowman, K. Takayama, N. A. Peppas and T. Nagai, *J. Controlled Release*, 1999, **61**, 329–335.
20 C.-M. Lehr, F. G. J. Poelma, H. E. Junginger and J. J. Tukker, *Int. J. Pharm.*, 1991, **70**, 235–240.
21 M. Kamiya, M. Matsumoto, K. Yamashita, T. Izumi, M. Kawaguchi, S. Mizukami, M. Tsurumaru, H. Mukai and S. Kawakami, *Pharmaceutics*, 2022, **14**, 2357.
22 J. Kristiansen, *Cryobiology*, 1992, **29**, 575–584.
23 H. Talsma, M. Van Steenbergen and D. Crommelin, *Int. J. Pharm.*, 1991, **77**, 119–126.
24 J. C. Kasper and W. Friess, *Eur. J. Pharm. Biopharm.*, 2011, **78**, 248–263.
25 J. Varshosaz, S. Eskandari and M. Tabbakhian, *Carbohydr. Polym.*, 2012, **88**, 1157–1163.
26 W. Wang, *Int. J. Pharm.*, 2000, **203**, 1–60.